Article

Impact of China's Permanent Basic Farmland Protection Redline and Ecological Protection Redline on Water Conservation in the Loess Gully Region

Jie Liu, Jizhe Zhou * and Qin He

School of Archtecture, Chang'an University, Xi'an 710061, China; 2023041005@chd.edu.cn (J.L.); 2022041001@chd.edu.cn (Q.H.)
* Correspondence: jizhezhou@chd.edu.cn

Abstract: Water conservation is crucial for sustainable ecosystem development in loess gully regions. The redlines of permanent basic farmland protection and ecological protection are key land use control zones in China, yet their impact on water conservation is understudied. The study focuses on Yan'an and constructs three scenarios: natural development (NDS), farmland protection (FPS), and ecological protection (EPS). Then, land use simulation for the three scenarios in 2025, 2030, and 2035 is carried out using the patch-generating land use simulation model. Finally, the integrated valuation of ecosystem services and trade-offs model is combined to calculate water conservation. The findings suggest the following: (1) From the temporal perspective, the water conservation of the three scenarios exhibits an incremental trend by period from 2025 to 2035, with an annual growth rate of approximately 0.65‰ for the NDS, 0.60‰ for the FPS, and 0.64‰ for the EPS. (2) From the scenario perspective, from 2025 to 2035, the annual water conservation under the FPS is 0.35‰ less than that under the NDS, while the impact of the EPS is weak at only ±0.1‰. (3) Across all scenarios, the average water conservation depth of grassland surpasses that of forestland. This study provides scientific evidence to help optimize China's land space governance policy as well as methodological and theoretical support for related studies.

Keywords: permanent basic farmland protection redline; ecological protection redline; water conservation; PLUS model; inVEST model; loess gully region

1. Introduction

Water conservation, as an important service function of terrestrial ecosystems, is a critical indicator for assessing the status of regional ecosystems [1,2]. In China, especially in loess gully regions with a fragile ecological environment and severe soil erosion, water conservation is indispensable for maintaining the regional ecological balance, preventing soil erosion, and underpinning economic development [3].

Reasonable land use policies are an effective approach to optimizing water conservation [4]. Thus, identifying the trends in ecosystem service changes induced by land use policies forms the scientific basis for policy optimization [5]. Relevant studies indicate that while land use policies may enhance certain services, they may also entail adverse consequences [6,7]. For instance, farmland consolidation may lead to issues such as soil and water pollution and biodiversity reduction [8,9]. Moreover, afforestation, despite its carbon sequestration benefits, might reduce water yield [10]. Therefore, the potential trade-offs between the ecosystem services provided by these policies and other services should be assessed across spatial and temporal scales [11].

Since November 2019, the Chinese government has promulgated the *Guiding Opinions on Coordinating and Implementing Three Control Lines in National Spatial Planning*, which strictly regulates land use conversions within the designated control areas. Although China's permanent basic farmland protection redline (PBFPR) and ecological protection

redline (EPR) were comprehensively delineated around 2017, these areas have been adjusted and redefined multiple times due to overlapping conflicts and implementation challenges [12–16]. Since 2020, these policies have become crucial elements in the spatial governance of the loess gully region and have been stringently enforced in practice.

While providing ecosystem services such as food supply and carbon sequestration, the policies of the permanent basic farmland protection redline and the ecological protection redline may also have profound impacts on water conservation services. Currently, research on these two redlines primarily focuses on the optimization of policy formulation [14,17–19] and delineation techniques [20–22]. In terms of policy impact assessment, many scholars concentrate on how farmland and ecological protection policies alter land use demands and how the changes in land use demands further affect ecosystem services [23–27]. In recent years, some studies have started to explore the impact of implementing the EPR on ecosystem services. For instance, Guo et al. evaluated the EPR in Guizhou Province and found that although the redline significantly reduced soil erosion and enhanced carbon sequestration, it may also lead to reduced water yield [12]. Nevertheless, research on the impacts of the PBFPR and EPR on water conservation remains insufficient, particularly in the unique loess gully region. Water conservation in this region is crucial for the sustainable development of the ecosystem.

Research on the impact of land use policies on ecosystem services often relies on land use simulation models to assess changes in ecosystem services. Commonly used land use change simulation models include the cellular automaton (CA) model [28,29], the CLUE-S model [30], the land transformation model (LTM) [31], the future land use simulation (FLUS) model [32,33] and the patch-generating land use simulation (PLUS) model [23,25,34]. For evaluating ecosystem services related to water conservation, notable models include the integrated valuation of ecosystem services and trade-offs (InVEST) model, the soil and water assessment tool (SWAT), and the artificial intelligence model of ecosystem services (ARIES). Studies have shown that the PLUS model offers higher simulation accuracy compared with other models [35,36]. Both the SWAT and InVEST models provide similar reference frameworks that can guide management and policy formulation [37]. The InVEST model is more suitable for the assessment of the influence of land use change on multiple ecosystem services [38]. Thus, the PLUS model is combined with the InVEST model with the purpose of obtaining the water yield. Meanwhile, the velocity coefficient, the terrain index, and the soil saturated hydraulic conductivity are adopted for calculating the water conservation.

Yan'an, as a typical loess gully region with broken topography and loose soil, is susceptible to water and wind erosion. Thus, there is a need to focus on its soil and water conservation. Consequently, this study selects Yan'an as the representative area. The specific objectives include: (1) simulating the land use in Yan'an in the natural development scenario (NDS), permanent basic farmland protection scenario (FPS), and ecological protection scenario (EPS) in 2025, 2030, and 2035; (2) calculating the spatial distribution of water yield and water conservation in Yan'an under these three scenarios in 2025, 2030, and 2035; and (3) investigating the impact of the PBFPR and the EPR on water conservation. The main contributions of this study include three aspects. First, it offers a basis for the optimization of land use policy zoning and water resource management in Yan'an. Second, it offers scientific support for the optimization of land use policies in the loess gully region. Third, it furnishes methodological references for simulating land use policies in other regions.

2. Materials and Methods

2.1. Study Area

As presented in Figure 1, Yan'an City is located in the northern part of Shaanxi Province, China, and is situated in the middle reaches of the Yellow River. It is a key area for soil and water conservation in the middle reaches of the Yellow River. It has jurisdiction over 13 districts and counties, with a total area of 37,000 square kilometers. The terrain is predominantly characterized by ridges and gullies, with an overall fragile

ecological environment and water resource scarcity. Between 2006 and 2022, the annual average precipitation was 554.9 mm, while the annual average potential evaporation was 1060.9 mm.
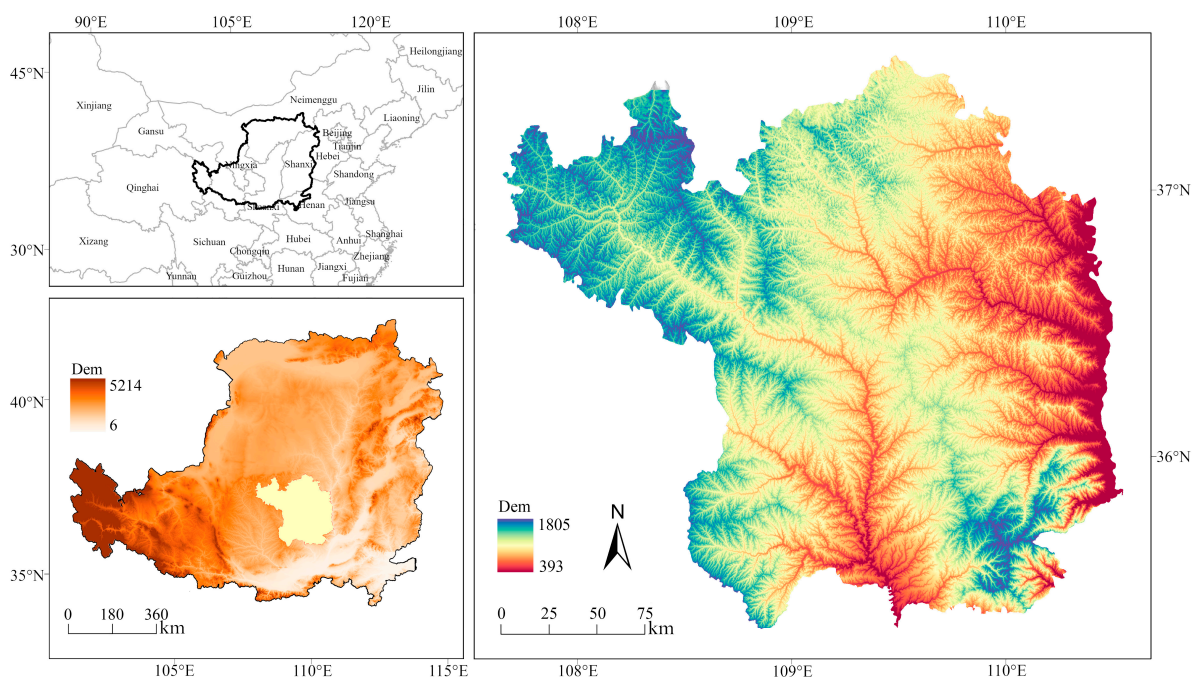

Figure 1. Location of the study area.

Yan'an City implements the strictest controls over the three control lines. In urbanized areas, the focus is on balancing development and conservation to guide the efficient concentration of economic, population, and innovation resources and to accelerate new-type industrialization and urbanization. In agricultural production areas, the policy prioritizes protection before development, with the primary aim of safeguarding farmland. In ecological function zones, the emphasis is on protecting the ecological environment while supporting the gradual and orderly migration of the population.

2.2. Data and Parameter Processing

Table 1 presents the foundational data for the PLUS model, while Table 2 outlines the basic data for the InVEST water yield module and the water conservation model. All raster data were resampled to a spatial resolution of 30 m using the ArcGIS Pro 3.0 software.

Table 1. Foundational data for the PLUS model.

Data	Spatial Resolution	Year	Data Resource
Land Use	30 m	2010, 2015, 2020	https://www.resdc.cn/ (accessed on 17 January 2024)
Dem	30 m	2019	http://www.gscloud.cn/ (accessed on 16 January 2024)
Slope	30 m	2019	http://www.gscloud.cn/ (accessed on 16 January 2024)
Annual Precipitation	1000 m	2020	https://data.tpdc.ac.cn/ (accessed on 26 January 2024)
Annual Evapotranspiration	1000 m	2020	https://data.tpdc.ac.cn/ (accessed on 26 January 2024)
Annual Mean Temperature	1000 m	2020	https://data.tpdc.ac.cn/ (accessed on 26 January 2024)

Table 1. *Cont.*

Data	Spatial Resolution	Year	Data Resource
Population	-	2020	*Yan'an Statistical Yearbook*
GDP	-	2020	*Yan'an Statistical Yearbook*
Distance from Roads of Various Levels	-	2020	https://www.resdc.cn/ (accessed on 26 January 2024)
PBFPR	-	-	*Yan'an Municipal Fourteenth Five-Year Plan for National Economic and Social Development and the Long-Range Objectives through to the Year 2035*
EPR	-	-	*Yan'an Municipal Fourteenth Five-Year Plan for National Economic and Social Development and the Long-Range Objectives through to the Year 2035*

Table 2. Foundational data for the InVEST model and the water conservation model.

Data	Spatial Resolution	Year	Data Resource
Average Annual Precipitation	1000 m	2006–2022	https://data.tpdc.ac.cn/ (accessed on 26 January 2024)
Average Annual Evapotranspiration	1000 m	2006–2022	https://data.tpdc.ac.cn/ (accessed on 26 January 2024)
Root-restricting Layer Depth	1000 m	2020	[39]
Plant-available Water Content	250 m	2017	https://data.isric.org/ (accessed on 7 February 2024)
Biophysical Table	-	-	[40,41]
Flow Velocity Coefficient	-	-	[42,43]
Soil Saturated Hydraulic Conductivity	250 m	2020	https://www.futurewater.eu/projects/hihydrosoil/ (accessed on 06 March January)

The foundational data for the PLUS model primarily include land use data, driving factor data, and spatial control data:

(1) Land use data: These data are obtained from the Resource and Environmental Science and Data Center of the Chinese Academy of Sciences and encompass 6 first-level types and 25 second-level types, with an overall accuracy of more than 90%. For simplification, some second-level types with smaller areas were merged into first-level types to form a final total of 6 first-level types and 16 second-level types. These specific types are as follows: cultivated land, which includes paddy fields (PF) and dry land (DL); forest land, which includes woodland (WL), shrub land (SHL), sparse woodland (SWL), and other woodland (OWL); grassland, which includes high-coverage grassland (HCG), medium-coverage grassland (MCG), and low-coverage grassland (LCG); water areas, which include rivers and ditches (RD), lakes (LK), reservoirs and ponds (RP), and floodplains (FLP); construction land, which includes urban construction land (UCL) and rural residential land (RRL); and unused land (UNL).

(2) Driving factor data: There are two topographic factors, namely dem and slope; three climate factors, namely annual precipitation, annual potential evapotranspiration, and annual average temperature; and eight socioeconomic factors, namely population, GDP, and the Euclidean distance to railways, highways, provincial roads, county roads, township roads, and county governments. The location data for county government offices were obtained using the reverse geocoding tool from Baidu Maps.

(3) Spatial control data: This involves the permanent basic farmland protection redline (PBFPR), the ecological protection redline (EPR), as well as the urban development boundary (UDB).

2.3. Research Method

The study establishes three scenarios: the natural development scenario (NDS), the permanent basic farmland protection scenario (FPS), and the ecological protection scenario

(EPS). In accordance with the spatial distribution of land use, water yield, and water conservation under the different scenarios in 2025, 2030, and 2035, the impact of implementing the PBFPR and EPR in the loess gully region is evaluated. The specific research framework can be found in Figure 2.
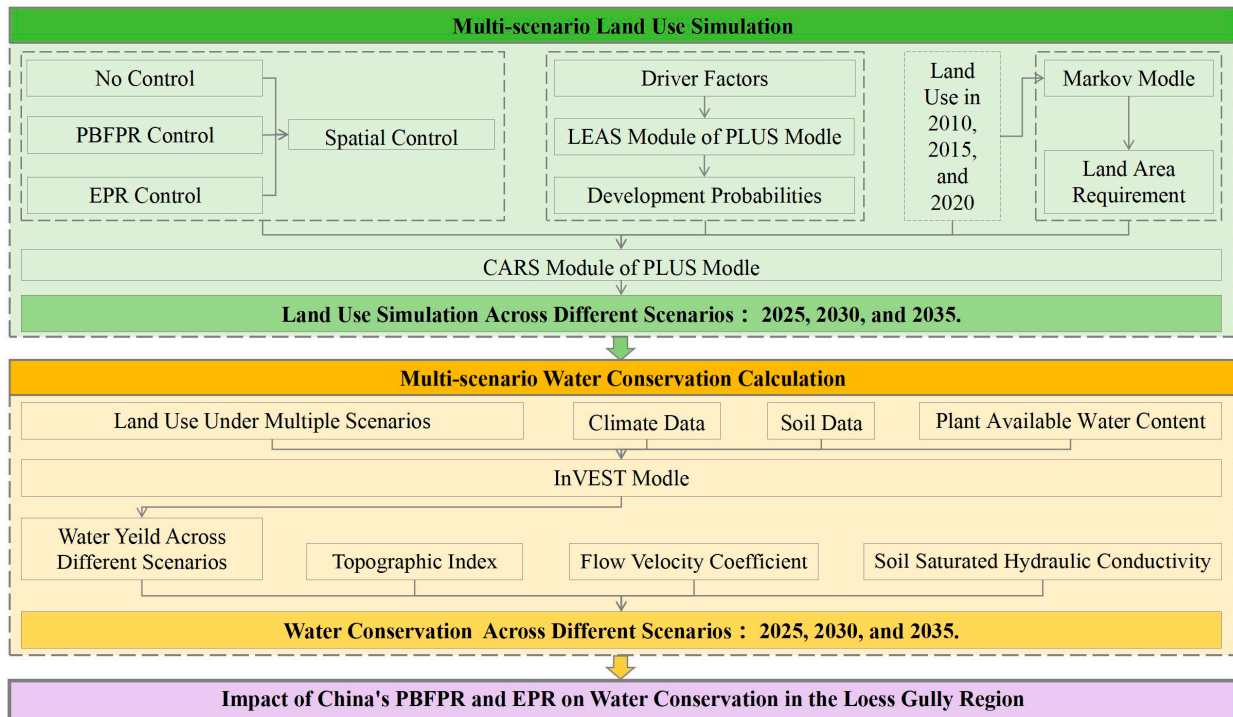

Figure 2. The workflow of this study.

2.3.1. The PLUS Model and Scenario Design

1. Land expansion strategy analysis

First, the transition data for various land uses from 2010 to 2015 were extracted. Then, the Land Expansion Analysis Strategy (LEAS) module was used to adopt the random forest algorithm to mine the driving factors of land transfer from the changing land use, and the development probability of each type of land use and the contribution of its driving factors were calculated. In this study, the sample sampling rate was defined as 0.1, the number of regression trees was 20, and the mTry number was 13.

2. Land demand prediction

To avoid interference in the evaluation results due to differences in land area demand under different scenarios, this study ensures that the goal of the land area demand is identical across the three scenarios. The Markov chain model was adopted for simulating land use demands for the years 2020, 2025, 2030, and 2035.

3. Land use simulation

In the CARS module, the simulation of land patch generation is carried out through combining random seed generation with a threshold decreasing mechanism. In this study, the neighborhood size was set to 3, the patch generation threshold to 0.5, the expansion coefficient to 0.1, and the percentage of random seeds to 0.0001. Based on the land expansion areas from 2015 and 2020, the neighborhood weights for each land type were calculated (Formula (1)), and the land use conversion matrix was set, where 0 represents non-convertible and 1 represents convertible.

$$H_i = \frac{|TA_i - TA_{min}|}{TA_{max} - TA_{min}} \tag{1}$$

where *Hi* denotes the neighborhood weight of the i-th land type, TA_i is the i-th land use transfer area, and TA_{min} and TA_{max} denote the minimum and maximum transition areas among all the land use types, respectively.

The "conversion restriction area" and "development zone" were set, with water bodies set as restricted areas (value 0), areas within the urban development boundary set as development zones (value 2), and all other areas assigned a value of 1. The development weight for the development zones was set to 0.5, and the development type was urban construction land code 14. Based on the land use data in 2015, this model successfully simulated the land use in 2020 (Figure 3), and the model's effectiveness was validated through accuracy verification, showing a Kappa coefficient of 0.85 and an overall accuracy of 88.31%.
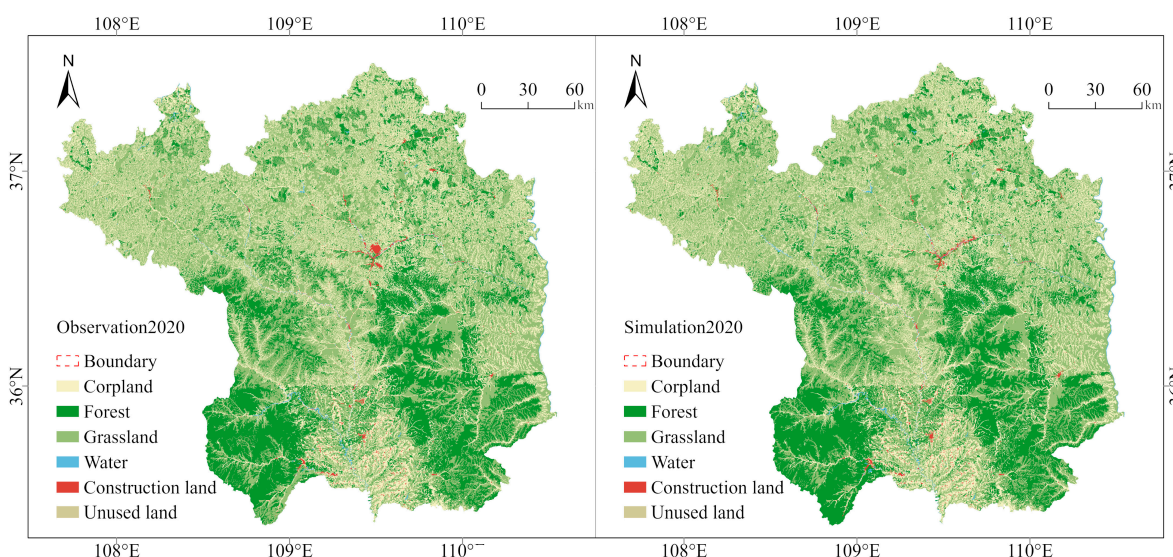

Figure 3. Comparison of the observed land use (**left**) versus the PLUS model simulation (**right**) for 2020.

4. Scenario design

This study sets three scenarios (Table 3). In the natural development scenario (NDS), water bodies are designated as restricted areas, while areas within the urban development boundary are designated as development zones. In the permanent basic farmland protection scenario (FPS), both water bodies and areas under the PBFPR are designated as restricted areas, while areas within the UDB are designated as development zones. In the ecological protection scenario (EPS), both water bodies and areas under the EPR are designated as restricted areas, while areas within the UDB are designated as development zones.

Table 3. Scenario design.

Scenario	Restricted Zones	Development Zones
NDS	Water	
FPS	Water, areas controlled by the PBFPR	Areas controlled by the UDB
EPS	Water, areas controlled by the EPR	

2.3.2. The InVEST Water Yield Model and Water Conservation

1. InVEST water yield model

The InVEST water yield model uses Formula (2) to calculate the water yield using the principle of the water cycle:

$$Y_j = \left(1 - \frac{AET_j}{P_j}\right) \times P_j \tag{2}$$

where Y_j is the annual water yield (mm); P_j is the annual average rainfall (mm); AET_j is the annual actual evapotranspiration (mm). The AET_j of the vegetation land use type is calculated using Formula (3), and the AET_j of other land types is calculated using Formula (4).

$$\frac{AET_j}{P_j} = \frac{1 + PET_j}{P_j} - \left[1 + \left(\frac{PET_j}{P_j}\right)^{W_j}\right]^{\frac{1}{W_j}} \tag{3}$$

$$AET_j = MIN(PET_j, P_j) \tag{4}$$

where PET_j is the potential evapotranspiration (mm), calculated using Formula (5); and W_j represents a dimensionless parameter that accounts for natural climatic and soil characteristics, calculated using Formula (6).

$$PET_j = KC_{ij} \times ET0_j \tag{5}$$

$$W_j = Z\frac{AWC_j}{P_j} + 1.25 \tag{6}$$

where $ET0_j$ is the evapotranspiration (mm); KC_{ij} denotes the plant evapotranspiration coefficient of land type i on grid j; AWC_j refers to the effective soil water content (%); and Z refers to the Zhang coefficient, which ranges from 1 to 30. According to the *Yan'an Water Resources Bulletin*, the average total water resource in Yan'an is 1.335 billion cubic meters. By inputting the multi-year average precipitation and evapotranspiration into the InVEST model and setting Z to 4.3, the calculated average total water resources for 2010, 2015, and 2020 is 1.373 billion cubic meters. This value closely approximates the average total water resources reported for Yan'an.

2.   Water conservation model

Relevant research indicates that water conservation is not only closely related to water yield but is also influenced by the soil characteristics, topography, and surface roughness. To fully account for the complex topographical features and spatial variability in the loess hilly region, this study first estimates water yield using a water yield module, and then calibrates this estimate by incorporating the topographic conditions, soil physical properties, and flow velocity. The final water conservation amount is calculated using Formula (7) [38,44]:

$$WR_j = MIN\left(1, \frac{249}{Vel_{ij}}\right) \times \left(1, \frac{0.9 \times T_j}{3}\right) \times \left(1, \frac{Ksat_j}{300}\right) \times Y_j \tag{7}$$

$$T_j = \log\left(\frac{Drainage\ Area}{Soil\ Depth \times Percent\ Slope}\right) \tag{8}$$

where WR_j represents the water conservation amount (mm); $Ksat_j$ represents the soil saturated hydraulic conductivity (mm/d); and Vel_{ij} is the velocity coefficient of land type i on grid unit j. T_j is the terrain index, which is dimensionless and calculated using Formula (8), and Y_j is the water yield, calculated via Formula (2). Given the significant alterations or degradation often associated with urban construction land, rural residential areas, and unused land, these parcels are set to Nodata. *Drainage Area* is the number of catchment grids, dimensionless; *Soil Depth* represents the soil depth (mm); and *Percent Slope* represents the percentage slope.

3. Results

3.1. Analysis of Land Use under Multiple Scenarios

3.1.1. Characteristics of Land Use Change from 2010 to 2035

Figure 4 illustrates the changes in the area in the various land use types from 2010 to 2035. Among the land use types that increased, medium-coverage grassland exhibited the largest growth, reaching 1194.92 square kilometers. This was followed by urban

construction land, which increased by 104.50 square kilometers. Other land types such as reservoirs and ponds, unused land, rivers and ditches, other woodlands, floodplains, and lakes also increased, though to a smaller extent. Conversely, among the land use types that decreased, dry land experienced the most significant reduction, shrinking by 578.82 square kilometers. This was followed by shrubland, which decreased by 381.82 square kilometers, and high-coverage grassland, which declined by 218.05 square kilometers. Additionally, low-coverage grassland, sparse woodland, woodland, rural residential land, and paddy fields also decreased, though to a smaller extent.
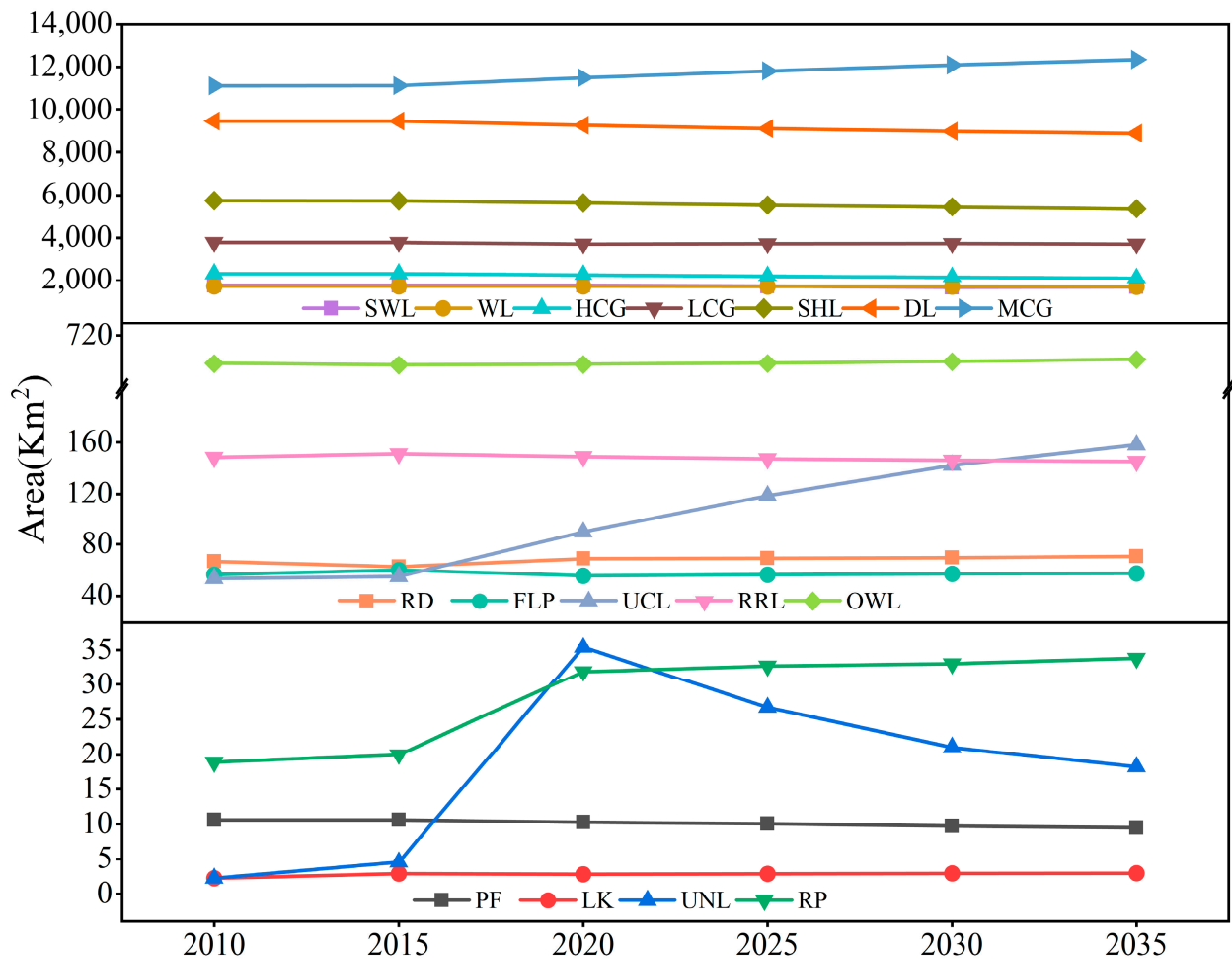

Figure 4. Area changes in the different land use types from 2010 to 2020.

3.1.2. Characteristics of Land Use Transfer

Figure 5 presents the proportion of the total land use transition area occupied by each land type. Across all three scenarios, there is a notable transition from dry land and shrubland to medium-coverage grassland. The combined transfer-out ratio of dry land and shrubland is approximately 45%, while the transfer-into ratio of medium-coverage grassland is also around 45%. Under the FPS, the transfer ratio of cultivated land is lower compared with that in the NDS. In the EPS, the transfer ratio of forest land is lower than that in the NDS. According to Figure 6, the spatial transition patterns of dry land, shrubland, and medium-coverage grassland are similar across the three scenarios.
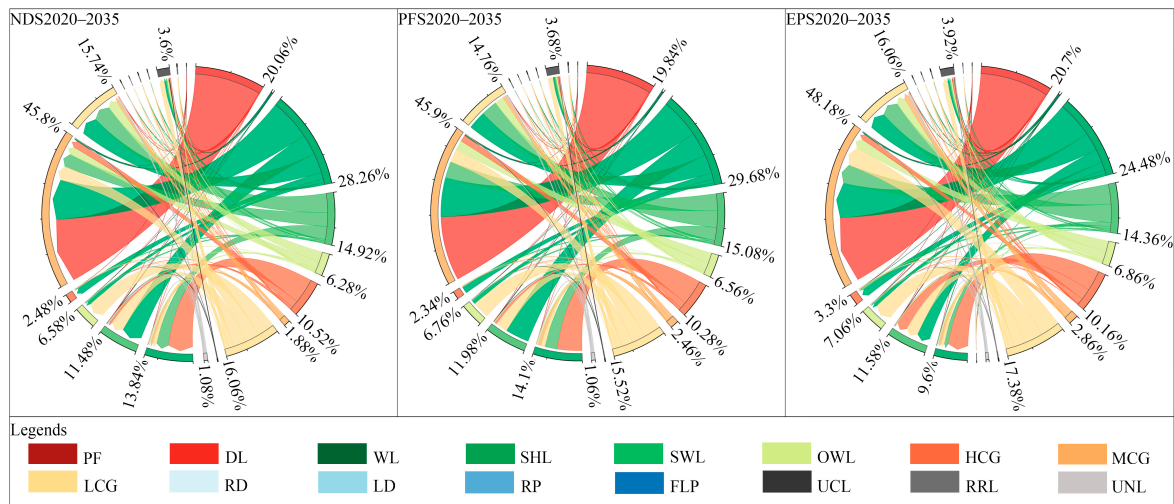
Figure 5. Proportions of land cover transitions under multiple scenarios for 2020–2035.
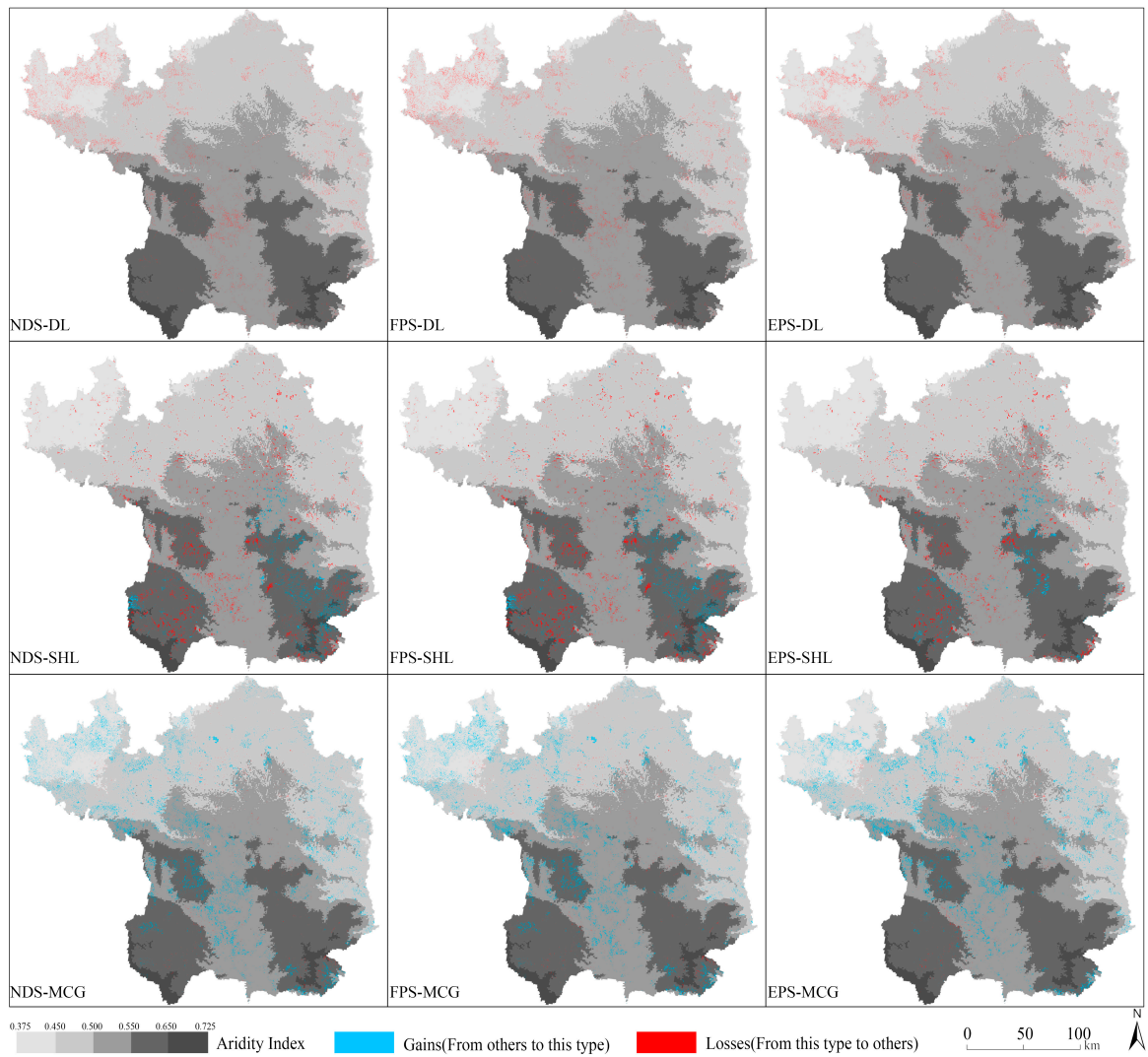

Figure 6. Spatial patterns of land use changes under multiple scenarios for 2020–2035.

3.2. Analysis of Water Yield and Water Conservation under Multiple Scenarios

3.2.1. Spatial Distribution of Water Yield and Water Conservation

As shown in Figure 7, the spatial distribution patterns of water yield and water conservation are similar across the three scenarios. The PBFPR and the EPR have a minimal effect on the spatial distribution pattern of water conservation in the study area. Clearly, the high values of water yield and water conservation are mainly distributed in areas with a drought index ranging from 0.501 to 0.550, while the low values of water yield and water conservation are mainly distributed in areas with a drought index of 0.375–0.450 and 0.551–0.650.
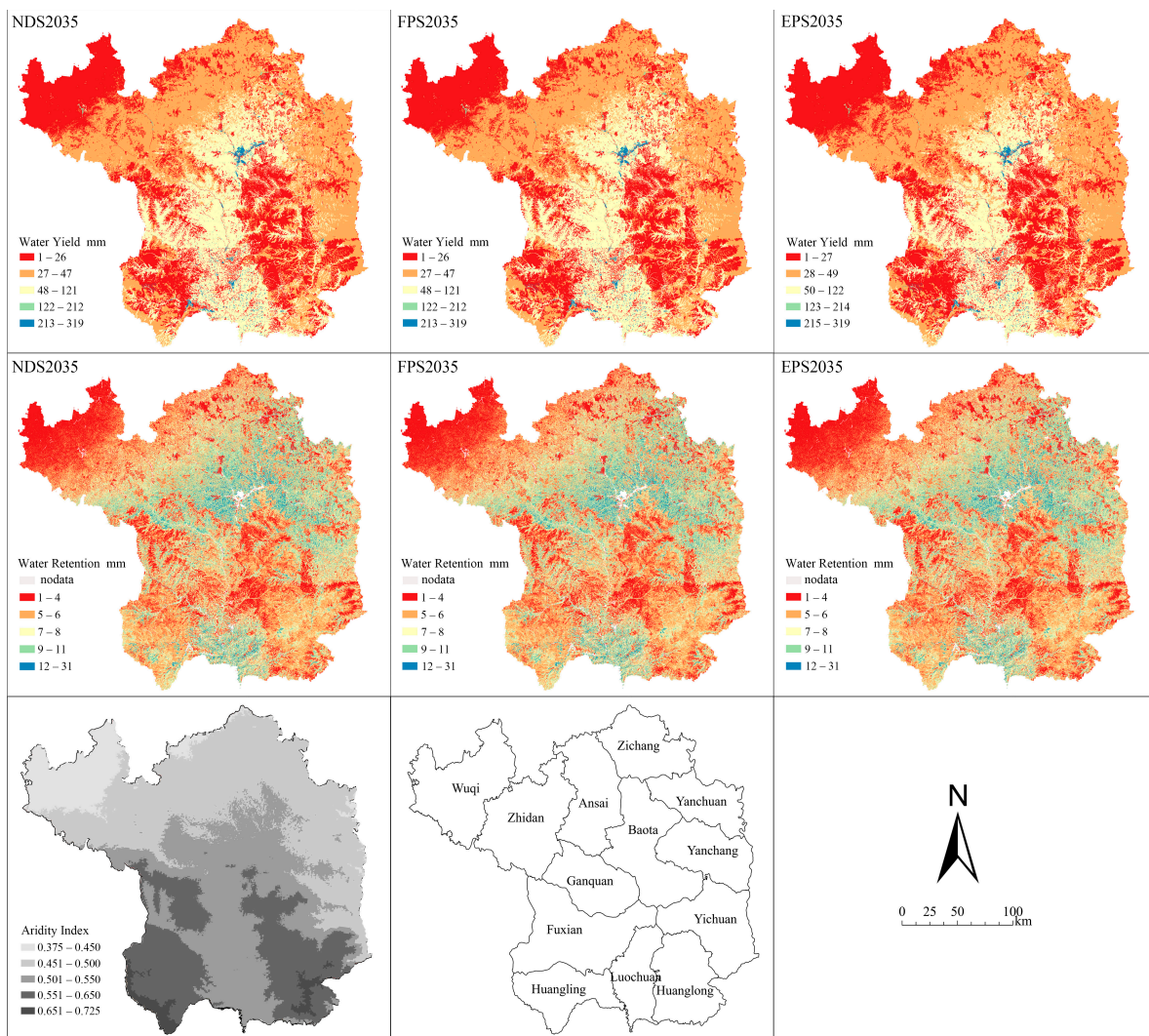

Figure 7. Spatial distribution of water yield and water conservation across multiple scenarios in 2035.

3.2.2. Water Yield Impact Analysis

Table 4 shows the changes in water yield in the time dimension and the multi-scenario dimension. In the time dimension, the water yield exhibits a trend of gradual increase. Under the NDS, the water yield increases from 1.392042 billion cubic meters in 2025 to 1.404349 billion cubic meters in 2035. In the FPS, the water yield increases from 1.391935 billion cubic meters in 2025 to 1.404342 billion cubic meters in 2035. Under the EPS, the water yield increases from 13.92007 billion cubic meters in 2025 to 14.04881 billion cubic meters in 2035.

Table 4. Water yield under multiple scenarios.

Year	Volume ($\times 10^8$ m³)		
	NDS	FPS	EPS
2020	13.83404	13.83404	13.83404
2025	13.92042	13.91935	13.92007
2030	14.00243	13.99798	14.00096
2035	14.04349	14.04342	14.04881

In the multi-scenario dimension, the water yield in the natural development scenario is consistently higher than that in the permanent basic farmland protection scenario across all periods. The latter scenario shows a decrease of approximately 0.1‰ on average per year compared with the former.

3.2.3. Water Conservation Impact Analysis

Table 5 shows the alterations in water conservation in the time dimension and multiple scenario dimensions. In terms of the time dimension, the average water conservation depth also shows a trend of gradual increase. Under the NDS, the average water conservation depth increases from 6.21091 mm in 2025 to 6.25153 mm in 2035. Under the FPS, the average water conservation depth increases from 6.21035 mm in 2025 to 6.24800 mm in 2035. Under the EPS, the average water conservation depth increases from 6.21157 mm in 2025 to 6.25113 mm in 2035. In the multi-scenario dimension, the water conservation depth in all three scenarios also exhibits a gradual upward trend. Specifically, the annual growth rate is approximately 0.65‰ in the NDS, about 0.60‰ in the FPS, and around 0.64‰ in the EPS.

Table 5. Average water conservation depth under multiple scenarios.

Year	Average Depth (mm)		
	NDS	FPS	EPS
2020	6.18275	6.18275	6.18275
2025	6.21091	6.21035	6.21157
2030	6.23698	6.23453	6.23678
2035	6.25153	6.24800	6.25113

In the multi-scenario dimension, the characteristics of the average water conservation depth are as follows: The average water conservation depth of the NDS is higher than that of the FPS in each period. Compared with the NDS, the average annual decrease of the FPS decreases by approximately 0.35‰ per year. The EPS exerts a weak effect on the average water conservation depth, with variations ranging around ±0.1‰.

Figure 8 presents the average water conservation depth for the various land use types across the different scenarios, which are ranked as follows: low-coverage grassland, medium-coverage grassland, high-coverage grassland, dry land, shrubland, woodland, sparse woodland, other woodland, and paddy fields. The specific values for the average water conservation depth under the NDS are as follows: paddy fields, 2.80394 mm; dry land, 5.55039 mm; woodland, 4.27190 mm; shrubland, 4.51460 mm; sparse woodland, 3.99649 mm; other woodland, 2.78409 mm; high-coverage grassland, 5.81327 mm; medium-coverage grassland, 7.15861 mm; and low-coverage grassland, 8.27530 mm. Under the FPS, the average water conservation depth of paddy fields and dry land increases, while the average water conservation depth of high-coverage grassland, medium-coverage grassland, and low-coverage grassland decreases.
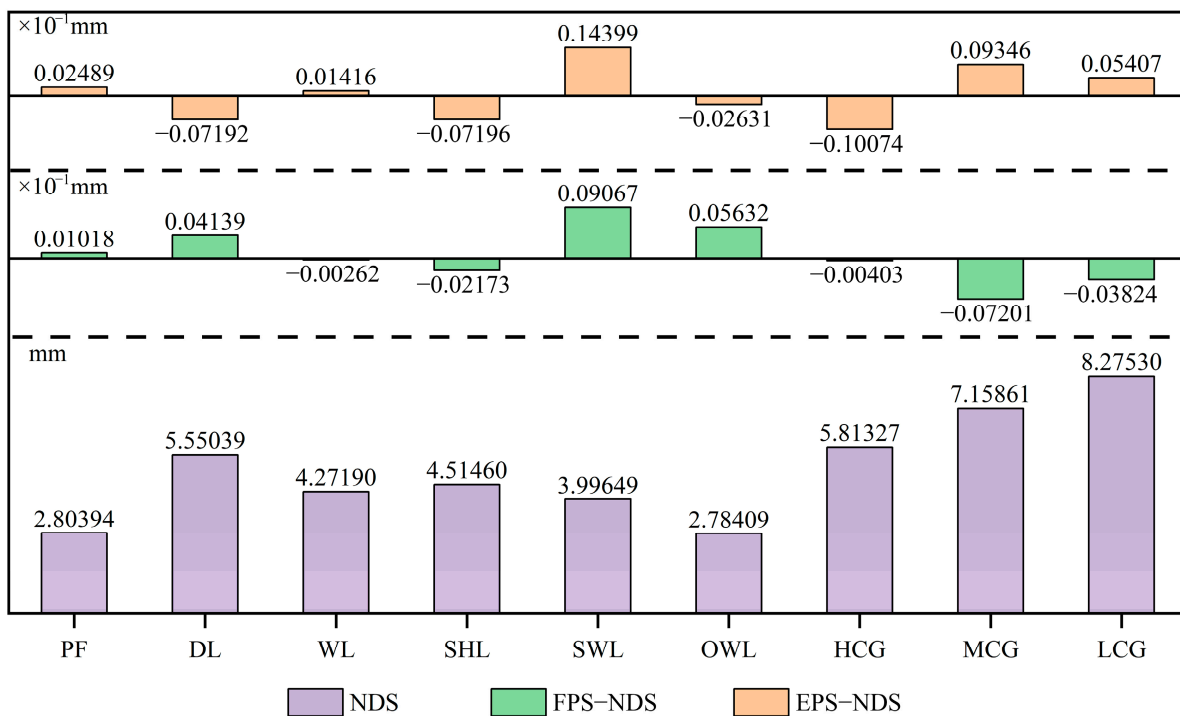
Figure 8. Average water conservation depth across land cover types under multiple scenarios in 2035.

4. Discussion

At present, hotspots in studies on the PBFPR and EPR mainly focus on the optimization of policy construction and demarcation technical methods. However, there is a relative paucity of studies evaluating the effectiveness of policy implementation. This study quantifies the long-term impacts of the PBFPR and the EPR on a key ecosystem service in the loess gully region, namely water conservation.

4.1. Discussion of the Impact of the PBFPR and EPR on Water Conservation

The research results indicate that in regions where the drought index ranges from 0.375 to 0.450 and 0.551 to 0.650, the water conservation capacity is relatively low. There is a strong spatial correlation between the spatial distribution of water conservation services and the drought index. Previous studies have shown that in the Loess Plateau, precipitation and vegetation are important factors affecting water conservation [44]. Particularly in arid regions where water resources are already scarce, afforestation increases evapotranspiration, and this consumption further exacerbates the water scarcity [45]. In areas with a drought index between 0.375 and 0.450, the precipitation is relatively low, while in regions with a drought index between 0.551 and 0.650, the forest cover is relatively high. Therefore, the reduction in water conservation in these two areas may be primarily attributed to insufficient precipitation and excessive forest cover, respectively.

The implementation of the policy for the PBFPR has resulted in a decrease in the overall water conservation service of about 0.35‰. More specifically, the average water conservation depth of cultivated land has increased, and the average water conservation depth of grassland has decreased. This may be because permanent basic farmland is mostly located in land areas with good soil quality and terrain conditions [46]. Restricting the conversion of these high-quality cultivated lands can suppress the enhancement of water conservation to a certain extent. Furthermore, related studies have indicated that cultivated land in the loess gully region exhibits serious fragmentation [47], poor fertility [48], and a low production potential [49]. Thus, it remains to be seen whether the value of food supply services provided by the permanent basic farmland protection policy can offset the loss in water conservation services.

The implementation of the EPR has a weak effect on water conservation in the study area. This may be caused by the evaluation models used during the delineation of the ecological redline not adequately considering spatial heterogeneity, resulting in the protected areas inherently lacking high water conservation capacity. According to the *Guidelines for the Delineation of Ecological Protection Redlines in China*, it is recommended that local governments give priority to the model assessment method. The model assessment method calculates the water conservation through the water balance equation, where the runoff volume is determined by applying the corresponding surface runoff coefficient values based on surface vegetation types. Although vegetation type is a significant factor influencing the surface runoff volume, it explains less than 50% of the surface runoff coefficients [50]. The surface runoff coefficient comprehensively reflects geological soil and vegetation conditions, and soil characteristics and topography are also important influencing factors [51]. Determining the surface runoff coefficient based only on the surface vegetation type is likely to cause deviations in the calculation results for areas with complex terrain like the loess gully region.

The study also indicated that the average water conservation amount of grassland is greater than that of forest land. Thus, grassland is more suitable for improving water conservation services in the loess gully region. This conclusion aligns with previous research findings: some studies utilizing multi-source datasets have demonstrated that while converting cropland to forest promotes soil retention, it diminishes the ecosystem's water conservation services [52]. Other studies have found through meta-analysis that in areas where farmland is returned to forests, these forests seriously deplete the soil water content compared with grassland and cultivated land [53]. Additionally, sampling data indicate that the annual soil water storage capacity of different vegetation types on the Loess Plateau decreases in the following order: naturally restored grassland, artificial grassland, cultivated land, artificial shrubland, and artificial woodland [54]. On loess slopes, the soil moisture in both artificial and natural forest lands is lower than in grasslands [55]. In addition, related studies have indicated that grasslands can better optimize the trade-off between maintaining runoff and soil erosion than forests [56].

4.2. Policy Optimization Suggestions for the Loess Gully Region

In the future land space governance and water resource management process of Yan'an, it may be beneficial to consider using the drought index as the basis for policy zoning. For areas with different drought levels, corresponding management and response policies should be formulated to improve the pertinence and effectiveness of these policies. Furthermore, the necessity of implementing the permanent basic farmland protection policy in the loess gully region should be evaluated through a more in-depth analysis. When delineating the ecological protection redline, local governments should refine parameters and models based on their unique terrain and landform characteristics, establishing ecological delineation rules suited to the local context. Additionally, it is recommended to prioritize the restoration of grasslands in the loess gully region during ecological restoration efforts.

4.3. Limitations and Future Work Suggestions

This study evaluated the impact of the PBFPR and the EPR policies on water conservation by integrating the PLUS model and the InVEST model. However, there are certain limitations to this research. Although the focus is on the impact of the two redline policies on water conservation, the underlying mechanisms of these impacts are still insufficiently understood. Therefore, future research should continue to delve into the intrinsic mechanisms behind these effects, aiming to provide more comprehensive policy recommendations for the optimization of land use policies.

5. Conclusions

To conclude, this study combines the PLUS model and the InVEST model to simulate the land use situation in Yan'an in 2025, 2030, and 2035 under the NDS, FPS, and EPS. Then,

the long-term impact of the PBFPR and the EPR on the key ecosystem service function of the loess gully region, namely water conservation, is evaluated. The findings show the following: (1) The PBFPR and the EPR have a weak effect on the spatial distribution pattern of water conservation. (2) The PBFPR somewhat suppresses the water conservation services in the study area. This indicates that there is a trade-off between farmland protection and water conservation in the study area. (3) The EPR has a limited impact on the water conservation service in the study area, potentially due to an inadequate consideration of spatial variability during its delineation. (4) Grassland is more conducive to water conservation services in the loess gully region. This finding aligns with previous research indicating that grasslands are more suitable for maintaining water conservation compared with forests.

Future research will focus on exploring the underlying mechanisms of the impacts of the PBFPR and EPR, as well as investigating how policy adjustments can further enhance water conservation. Additionally, assessments of land use policies in various regions will provide broader insights. This study lays the foundation for policy optimization and offers valuable methodological insights for future research.

Author Contributions: Conceptualization, data curation, writing—original draft preparation, visualization, writing—reviewing and editing, J.L.; methodology, supervision, project administration, J.Z.; software and validation, Q.H. All authors have read and agreed to the published version of the manuscript.

Data Availability Statement: The original contributions presented in the study are included in the article, further inquiries can be directed to the corresponding author.

Conflicts of Interest: The authors declare no conflicts of interest.

References

1. Xue, J.; Li, Z.; Feng, Q.; Gui, J.; Zhang, B. Spatiotemporal Variations of Water Conservation and Its Influencing Factors in Ecological Barrier Region, Qinghai-Tibet Plateau. *J. Hydrol. Reg. Stud.* **2022**, *42*, 101164. [CrossRef]
2. Zuo, D.; Chen, G.; Wang, G.; Xu, Z.; Han, Y.; Peng, D.; Pang, B.; Abbaspour, K.C.; Yang, H. Assessment of Changes in Water Conservation Capacity under Land Degradation Neutrality Effects in a Typical Watershed of Yellow River Basin, China. *Ecol. Indic.* **2023**, *148*, 110145. [CrossRef]
3. Liu, Y.; Liu, X.; Zhang, B. Spatial Features Analysis of Water Conservation Function in the Hilly Areas of the Loess Plateau Based on InVEST Model. *Acta Ecol. Sin.* **2020**, *40*, 6161–6170. [CrossRef]
4. Vandecasteele, I.; Marí i Rivero, I.; Baranzelli, C.; Becker, W.; Dreoni, I.; Lavalle, C.; Batelaan, O. The Water Retention Index: Using Land Use Planning to Manage Water Resources in Europe. *Sustain. Dev.* **2018**, *26*, 122–131. [CrossRef]
5. Yang, Y.; Yuan, X.; An, J.; Su, Q.; Chen, B. Drivers of Ecosystem Services and Their Trade-Offs and Synergies in Different Land Use Policy Zones of Shaanxi Province, China. *J. Clean. Prod.* **2024**, *452*, 142077. [CrossRef]
6. Cord, A.F.; Bartkowski, B.; Beckmann, M.; Dittrich, A.; Hermans-Neumann, K.; Kaim, A.; Lienhoop, N.; Locher-Krause, K.; Priess, J.; Schröter-Schlaack, C.; et al. Towards Systematic Analyses of Ecosystem Service Trade-Offs and Synergies: Main Concepts, Methods and the Road Ahead. *Ecosyst. Serv.* **2017**, *28*, 264–272. [CrossRef]
7. Shi, M.; Wu, H.; Fan, X.; Jia, H.; Dong, T.; He, P.; Baqa, M.F.; Jiang, P. Trade-Offs and Synergies of Multiple Ecosystem Services for Different Land Use Scenarios in the Yili River Valley, China. *Sustainability* **2021**, *13*, 1577. [CrossRef]
8. Zhong, L.; Wang, J.; Zhang, X.; Ying, L. Effects of Agricultural Land Consolidation on Ecosystem Services: Trade-Offs and Synergies. *J. Clean. Prod.* **2020**, *264*, 121412. [CrossRef]
9. Wang, J.; Yan, S.; Guo, Y.; Li, J.; Sun, G. The Effects of Land Consolidation on the Ecological Connectivity Based on Ecosystem Service Value: A Case Study of Da'an Land Consolidation Project in Jilin Province. *J. Geogr. Sci.* **2015**, *25*, 603–616. [CrossRef]
10. Nosetto, M.D.; Jobbágy, E.G.; Brizuela, A.B.; Jackson, R.B. The Hydrologic Consequences of Land Cover Change in Central Argentina. *Agric. Ecosyst. Environ.* **2012**, *154*, 2–11. [CrossRef]
11. Viglizzo, E.F.; Paruelo, J.M.; Laterra, P.; Jobbágy, E.G. Ecosystem Service Evaluation to Support Land-Use Policy. *Agric. Ecosyst. Environ.* **2012**, *154*, 78–84. [CrossRef]
12. Guo, X.; Zhang, Y.; Guo, D.; Lu, W.; Xu, H. How Does Ecological Protection Redline Policy Affect Regional Land Use and Ecosystem Services? *Environ. Impact Assess. Rev.* **2023**, *100*, 107062. [CrossRef]

13. Jiang, B.; Bai, Y.; Wong, C.P.; Xu, X.; Alatalo, J.M. China's Ecological Civilization Program–Implementing Ecological Redline Policy. *Land Use Policy* **2019**, *81*, 111–114. [CrossRef]
14. Wang, N.; Hao, J.; Zhang, L.; Duan, W.; Shi, Y.; Zhang, J.; Wusimanjiang, P. Basic Farmland Protection System in China: Changes, Conflicts and Prospects. *Agronomy* **2023**, *13*, 651. [CrossRef]
15. Xu, X.; Tan, Y.; Yang, G.; Barnett, J. China's Ambitious Ecological Red Lines. *Land Use Policy* **2018**, *79*, 447–451. [CrossRef]
16. Zhou, Y.; Li, X.; Liu, Y. Cultivated Land Protection and Rational Use in China. *Land Use Policy* **2021**, *106*, 105454. [CrossRef]
17. Qie, L.; Pu, L.; Tang, P.; Liu, R.; Huang, S.; Xu, F.; Zhong, T. Gains and Losses of Farmland Associated with Farmland Protection Policy and Urbanization in China: An Integrated Perspective Based on Goal Orientation. *Land Use Policy* **2023**, *129*, 106643. [CrossRef]
18. Qiu, T.; Luo, B.; Li, S.; He, Q. Does the Basic Farmland Preservation Hinder Land Transfers in Rural China? *China Agric. Econ. Rev.* **2019**, *12*, 39–56. [CrossRef]
19. Bai, Y.; Wong, C.P.; Jiang, B.; Hughes, A.C.; Wang, M.; Wang, Q. Developing China's Ecological Redline Policy Using Ecosystem Services Assessments for Land Use Planning. *Nat. Commun.* **2018**, *9*, 3034. [CrossRef]
20. Chen, Y.; Yao, M.; Zhao, Q.; Chen, Z.; Jiang, P.; Li, M.; Chen, D. Delineation of a Basic Farmland Protection Zone Based on Spatial Connectivity and Comprehensive Quality Evaluation: A Case Study of Changsha City, China. *Land Use Policy* **2021**, *101*, 105145. [CrossRef]
21. Chen, D.; Pan, Y.; Jin, X.; Du, H.; Li, M.; Jiang, P. The Delineation of Ecological Redline Area for Catchment Sustainable Management from the Perspective of Ecosystem Services and Social Needs: A Case Study of the Xiangjiang Watershed, China. *Ecol. Indic.* **2021**, *121*, 107130. [CrossRef]
22. Zhang, Y.; Yang, B.; Liu, Y.; Wu, S.; Cui, Y.; Xu, T. High-Precision Ecological Protection Red Line Boundary Optimization for Fangshan District, Beijing, China. *Sens. Mater.* **2023**, *35*, 835. [CrossRef]
23. Gao, L.; Tao, F.; Liu, R.; Wang, Z.; Leng, H.; Zhou, T. Multi-Scenario Simulation and Ecological Risk Analysis of Land Use Based on the PLUS Model: A Case Study of Nanjing. *Sustain. Cities Soc.* **2022**, *85*, 104055. [CrossRef]
24. Liu, K.; Zhang, C.; Zhang, H.; Xu, H.; Xia, W. Spatiotemporal Variation and Dynamic Simulation of Ecosystem Carbon Storage in the Loess Plateau Based on PLUS and InVEST Models. *Land* **2023**, *12*, 1065. [CrossRef]
25. Liu, X.; Liu, Y.; Wang, Y.; Liu, Z. Evaluating Potential Impacts of Land Use Changes on Water Supply–Demand under Multiple Development Scenarios in Dryland Region. *J. Hydrol.* **2022**, *610*, 127811. [CrossRef]
26. Xiong, M.; Li, F.; Liu, X.; Liu, J.; Luo, X.; Xing, L.; Wang, R.; Li, H.; Guo, F. Characterization of Ecosystem Services and Their Trade-Off and Synergistic Relationships under Different Land-Use Scenarios on the Loess Plateau. *Land* **2023**, *12*, 2087. [CrossRef]
27. Cui, L.; Tang, W.; Zheng, S.; Singh, R.P. Ecological Protection Alone Is Not Enough to Conserve Ecosystem Carbon Storage: Evidence from Guangdong, China. *Land* **2023**, *12*, 111. [CrossRef]
28. Sang, L.; Zhang, C.; Yang, J.; Zhu, D.; Yun, W. Simulation of Land Use Spatial Pattern of Towns and Villages Based on CA–Markov Model. *Math. Comput. Model.* **2011**, *54*, 938–943. [CrossRef]
29. Wang, S.Q.; Zheng, X.Q.; Zang, X.B. Accuracy Assessments of Land Use Change Simulation Based on Markov-Cellular Automata Model. *Procedia Environ. Sci.* **2012**, *13*, 1238–1245. [CrossRef]
30. Jiang, W.; Chen, Z.; Lei, X.; Jia, K.; Wu, Y. Simulating Urban Land Use Change by Incorporating an Autologistic Regression Model into a CLUE-S Model. *J. Geogr. Sci.* **2015**, *25*, 836–850. [CrossRef]
31. Pijanowski, B.C.; Brown, D.G.; Shellito, B.A.; Manik, G.A. Using Neural Networks and GIS to Forecast Land Use Changes: A Land Transformation Model. *Comput. Environ. Urban Syst.* **2002**, *26*, 553–575. [CrossRef]
32. Lin, W.; Sun, Y.; Nijhuis, S.; Wang, Z. Scenario-Based Flood Risk Assessment for Urbanizing Deltas Using Future Land-Use Simulation (FLUS): Guangzhou Metropolitan Area as a Case Study. *Sci. Total Environ.* **2020**, *739*, 139899. [CrossRef]
33. Zhang, Y.; Yu, P.; Tian, Y.; Chen, H.; Chen, Y. Exploring the Impact of Integrated Spatial Function Zones on Land Use Dynamics and Ecosystem Services Tradeoffs Based on a Future Land Use Simulation (FLUS) Model. *Ecol. Indic.* **2023**, *150*, 110246. [CrossRef]
34. Wang, Q.; Guan, Q.; Sun, Y.; Du, Q.; Xiao, X.; Luo, H.; Zhang, J.; Mi, J. Simulation of Future Land Use/Cover Change (LUCC) in Typical Watersheds of Arid Regions under Multiple Scenarios. *J. Environ. Manag.* **2023**, *335*, 117543. [CrossRef]
35. Liang, X.; Guan, Q.; Clarke, K.C.; Liu, S.; Wang, B.; Yao, Y. Understanding the Drivers of Sustainable Land Expansion Using a Patch-Generating Land Use Simulation (PLUS) Model: A Case Study in Wuhan, China. *Comput. Environ. Urban Syst.* **2021**, *85*, 101569. [CrossRef]
36. Wang, J.; Zhang, J.; Xiong, N.; Liang, B.; Wang, Z.; Cressey, E.L. Spatial and Temporal Variation, Simulation and Prediction of Land Use in Ecological Conservation Area of Western Beijing. *Remote Sens.* **2022**, *14*, 1452. [CrossRef]
37. Cong, W.; Sun, X.; Guo, H.; Shan, R. Comparison of the SWAT and InVEST Models to Determine Hydrological Ecosystem Service Spatial Patterns, Priorities and Trade-Offs in a Complex Basin. *Ecol. Indic.* **2020**, *112*, 106089. [CrossRef]
38. Li, M.; Liang, D.; Xia, J.; Song, J.; Cheng, D.; Wu, J.; Cao, Y.; Sun, H.; Li, Q. Evaluation of Water Conservation Function of Danjiang River Basin in Qinling Mountains, China Based on InVEST Model. *J. Environ. Manag.* **2021**, *286*, 112212. [CrossRef] [PubMed]
39. Yan, F.; Shangguan, W.; Zhang, J.; Hu, B. Depth-to-Bedrock Map of China at a Spatial Resolution of 100 Meters. *Sci. Data* **2020**, *7*, 2. [CrossRef]
40. Yang, J.; Xie, B.; Zhang, D. Spatio-Temporal Variation of Water Yield and Its Response to Precipitation and Land Use Change in the Yellow River Basin Based on InVEST Model. *Chin. J. Appl. Ecol.* **2020**, *31*, 2731–2739. [CrossRef]

41. Yu, C.; Huang, X.; Guo, Q.; Yang, Y.; Xu, Z. Predicting Water Ecosystem Services under Prospective Climate and Land-Use Change Scenarios in Typical Watersheds Distributed across China. *Ecol. Indic.* **2024**, *159*, 111744. [CrossRef]
42. Bao, Y.; Li, T.; Liu, H.; Ma, T.; Wang, H.; Liu, K.; Shen, X.; Liu, X. Spatial and Temporal Changes of Water Conservation of Loess Plateau in Northern Shaanxi Province by InVEST Model. *Geogr. Res.* **2016**, *35*, 664–676. [CrossRef]
43. Chen, S. Evaluation of Ecological Service Function of Water Retention and Soil Conservation in Water Source Area for the South-to-North Water Transfer: A Case Study in Shangluo City. Ph.D. Thesis, Northwest University, Xi'an, China, 2016.
44. Xu, H.; Zhao, C.; Wang, X.; Chen, S.; Shan, S.; Chen, T.; Qi, X. Spatial Differentiation of Determinants for Water Conservation Dynamics in a Dryland Mountain. *J. Clean. Prod.* **2022**, *362*, 132574. [CrossRef]
45. Zan, B.; Ge, J.; Mu, M.; Sun, Q.; Luo, X.; Wei, J. Spatiotemporal Inequality in Land Water Availability Amplified by Global Tree Restoration. *Nat. Water* **2024**, 1–12. [CrossRef]
46. Qianwen, C.; Penghui, J.; Lingyan, C.; Jinxia, S.; Yunqian, Z.; Liyan, W.; Manchun, L.; Feixue, L.; Axing, Z.; Dong, C. Delineation of a Permanent Basic Farmland Protection Area around a City Centre: Case Study of Changzhou City, China. *Land Use Policy* **2017**, *60*, 73–89. [CrossRef]
47. Wang, Z.; Wu, J.; Bai, S.; Wang, H.; Chen, Y. Evaluation of Cultivated Land Fragmentation and Land Consolidation Engineering Zoning in the Loess Hilly and Gully Region: A Case Study in Wuqi County. *Res. Soil Water Conserv.* **2022**, *29*, 300–307.
48. He, J.; Bai, H.; Wang, J.; Xu, Y.; Ni, L. Spatial Patterns and Driving Factors of Soil Nutrient Contents in Cultivated Lands Across Various Topographical Types in the Loess Plateau. *Res. Soil Water Conserv.* **2024**, *31*, 1–11. [CrossRef]
49. Xu, Q.; Yang, G.; Gu, W.; Xie, T.; Liu, R. Estimation of Potential Productivity over Arable Land in Shaanxi Province of West China. *Remote Sens. Inf.* **2017**, *32*, 141–151.
50. Gong, S.; Xiao, Y.; Fang, Y.; Zheng, H.; Xiao, Y.; Ouyang, Z. Forest Ecosystem Surface Run-off Regulation Characteristics in China. *Acta Ecol. Sin.* **2016**, *36*, 7472–7478.
51. Kong, W.; Zhou, B.; Fu, M.; Li, Z.; Xie, J.; Wu, M. Effects of Different Land-Use on Characteristics of Soil and Water Conservation. *Joumal Nanjng For. Univ. (Nat. Sci. Ed.)* **2009**, *33*, 57–61.
52. Jiang, C.; Zhang, H.; Wang, X.; Feng, Y.; Labzovskii, L. Challenging the Land Degradation in China's Loess Plateau: Benefits, Limitations, Sustainability, and Adaptive Strategies of Soil and Water Conservation. *Ecol. Eng.* **2019**, *127*, 135–150. [CrossRef]
53. Li, B.; Zhang, W.; Li, S.; Wang, J.; Liu, G.; Xu, M. Severe Depletion of Available Deep Soil Water Induced by Revegetation on the Arid and Semiarid Loess Plateau. *For. Ecol. Manag.* **2021**, *491*, 119156. [CrossRef]
54. Ge, F. The Water Conservation Function of Typical Artificial Vegetation on the Loess Plateau of China. Ph.D. Thesis, Northwest A&F University, Xianyang, China, 2023.
55. Mei, X.; Ma, L.; Zhu, Q.; Wang, S.; Zhang, D.; Wang, Y. Responses of Soil Moisture to Vegetation Restoration Type and Slope Length on the Loess Hillslope. *J. Mt. Sci.* **2018**, *15*, 548–562. [CrossRef]
56. Liu, Y.; Dunkerley, D.; López-Vicente, M.; Shi, Z.-H.; Wu, G.-L. Trade-off between Surface Runoff and Soil Erosion during the Implementation of Ecological Restoration Programs in Semiarid Regions: A Meta-Analysis. *Sci. Total Environ.* **2020**, *712*, 136477. [CrossRef]